THE JOURNAL OF BIOLOGICAL CHEMISTRY
Vol. 276, No. 49, Issue of December 7, pp. 46268–46275, 2001

*Printed in U.S.A.*

# A Protein G Fragment from the Salmonid Viral Hemorrhagic Septicemia Rhabdovirus Induces Cell-to-Cell Fusion and Membrane Phosphatidylserine Translocation at Low pH*

Received for publication, September 10, 2001, and in revised form, September 21, 2001
Published, JBC Papers in Press, October 4, 2001, DOI 10.1074/jbc.M108682200

**Amparo M. Estepa‡, Ana I. Rocha§, Vicente Mas‡, Luis Pérez‡, Jose Antonio Encinar‡, Elena Nuñez¶, Asia Fernandez‡, Jose Manuel Gonzalez Ros¶, Francisco Gavilanes¶, and Julio M. Coll§‖**

*From the ‡Centro Biología Molecular y Celular, Universidad Miguel Hernandez, Elche, Spain 03202, ¶Departmento Bioquimica, Universidad Complutense de Madrid, Madrid, Spain 28028, and §Instituto Nacional Investigaciones Agrarias y Alimentar, Subdireccion General Investigacion y Tecnologia, Departmento Biotecnología, Crt. Coruña Km 7, Madrid 28040, Spain*

**The fusion-related properties of segments p9, p3, p4, and p9 + p2 surrounding the p2 phospholipid-binding domain of the protein G (pG) of the salmonid rhabdovirus of viral hemorrhagic septicemia (VHS) (Nuñez, E., Fernandez, A. M., Estepa, A., Gonzalez-Ros, J. M., Gavilanes, F., and Coll, J. M. (1998) *Virology* 243, 322–330; Estepa, A., and Coll, J. M. (1996) *Virology* 216, 60–70), have been studied at neutral and fusion (low) pH values by using its derived peptides. Cell-to-cell fusion, translocation of phosphatidylserine, and inhibition of fusion of pG-transfected cells defined the p9 + p2 (fragment 11, sequence 56–110) as a fragment with higher specific activity for anionic phospholipid aggregation than the previously reported p2. While fragment 11, p2, and p3 showed interactions with anionic phospholipids, p9 and p4 showed no interactions with any phospholipids. When added to a cell monolayer model at low pH, fragment 11 induced pH-dependent cell-to-cell fusion and translocated phosphatidylserine from the inner to the outer leaflet of the membrane. At low pH and in the presence of anionic phospholipids, fragment 11 showed more than 80% β-sheet conformation (IR and CD spectroscopies). Finally, anti-fragment 11 antibodies inhibited low pH-dependent pG-transfected cell-to-cell fusion. All of the data support the conclusion that fragment 11 is a primary determinant of some of the viral cell fusion events in VHSV.**

The protein G (pG)[1] of mammalian and fish rhabdoviruses have (500 amino acids. The pG contains 2–6 glycosylation sites, 6–8 highly conserved disulfide bridges (3, 4), two or three noncanonical hydrophobic heptad repeats (5), a carboxyl transmembrane region, a carboxyl-terminal cytoplasmic domain, and a removed signal peptide (6) (Fig. 1*A*). The pG forms homotrimers to bind to the host cell receptor(s) and after endocytosis fuses with the host membranes (7), following structural rearrangements triggered by the low pH of the endosome (8). Contrary to many other enveloped viruses, in rhabdoviruses there is no proteolytic processing of pG to expose a fusion domain (the so-called fusion peptide). Furthermore, the putative fusion domain is not hydrophobic but neutral, it contains an internal cysteine (except in rabies virus) (9, 10), and at least some of the conformational changes required for low pH fusion are reversible (11). Fusion-defective mutants in vesicular stomatitis virus (10, 12) and neutralizing monoclonal antibody (mAb)-resistant mutants at low pH in rabies virus (13) identified fusion-related domains in these rhabdoviruses. An alignment model based in highly conserved cysteines identified homologous putative fusion domains in other 14 animal rhabdoviruses (3). However, there is not yet a mechanism or model to explain how fusion occurs in these viruses; nor has a complete fusion-defective mutant screening been performed to map all possible fusion-related functional domains (14). All of the above mentioned data make rhabdoviral fusion an intriguing subject to study viral entry in cells.

The major anionic phospholipid-binding domain of the pG (p2, sequence 82–109) of viral hemorrhagic septicemia virus (VHSV), a rhabdovirus of salmonids (15, 16), is related to fusion after VHSV binding to its cell receptors (17, 18). For instance, anti-p2 antibodies (Abs) inhibited phospholipid binding to VHSV (2) and VHSV-induced cell-to-cell fusion (19). In addition, p2 mediates phospholipid vesicle fusion, lipid mixing, and leakage of liposome contents and inserts itself into liposome membranes by adopting a β-sheet structure (1). Furthermore, phospholipid binding to VHSV (2) and fusion of pG gene-transfected cells (20) showed similar pH-dependent profiles. However, the location of the phospholipid-binding domain (sequence 82–109) (15) and the location of the putative fusion domain (sequence 142–156) (3) are separated in pG. On the other hand, based on mutants changing the fusion pH, it has been suggested that the complete fusion structure of VHSV could be constituted by two distant pG domains situated around sequences 110–118 and 144–154 (21). These sequences are maintained together by a disulfide bond between $Cys^{110}$ and $Cys^{152}$ (4).

We selected four segments surrounding the p2 phospholipid-binding domain and located upstream of the putative fusion domain to study its possible relationship with fusion in the

* This work was supported by the FAIR Program of the European Economic Community (Grants CT98-4003 and CT98-4398), Comisión Interministerial de Ciencia y Tecnología (Spain) Project AGF98-580, INIA project SC00046, and the Comunidad Valenciana CV98-10-33 project. The costs of publication of this article were defrayed in part by the payment of page charges. This article must therefore be hereby marked "*advertisement*" in accordance with 18 U.S.C. Section 1734 solely to indicate this fact.

‖ To whom correspondence should be addressed. Tel.: 34-1-3476850; Fax: 34-1-3572293; E-mail: coll@inia.es.

[1] The abbreviations used are: pG, protein G; VHSV, viral hemorrhagic septicemia virus; Ab, antibody; mAb, monoclonal Ab; p2, phospholipid-binding domain; PS, phosphatidylserine; PI, phosphatidylinositol; PIPP, phosphatidylinositol bisphosphate; PrIo, propidium iodide; EPC, epithelial papullosum cyprini; FITC, fluorescein isothiocyanate; MES, 4-morpholineethanesulfonic acid.

VHSV model. The selected segments were p9 (sequence 58–80), p3 (sequence 110–122), p4 (sequence 123–144), and fragment 11 (p9 + p2, fragment 11 from sequence 56–110) (Fig. 1, *A* and *B*). We then used synthetic or recombinant peptides derived from them to study their fusion-related properties at neutral and fusion (low pH). While fragment 11, p2, and p3 showed interactions with anionic phospholipids, p9 and p4 showed no interactions with any phospholipids. At the low pH of fusion, fragment 11 showed the highest anionic phospholipid binding specific activity and was unique in inducing noninfected cell-to-cell fusion and translocating phosphatidylserine (PS) from the inner to the outer leaflet of the membrane. Fragment 11 required low pH for most of its activities and at that pH showed a complete β-sheet structure. Finally, anti-fragment 11 inhibition of pG-transfected cell fusion confirmed the implication of fragment 11 in fusion of pG with cellular membranes. All the above mentioned data shows that fragment 11 participates in VHSV-cell fusion.

## MATERIALS AND METHODS

*Analysis of the pG of Rhabdoviruses*—The alignment model proposed for cDNA-derived pG sequences of 14 animal rhabdoviruses belonging to four genera (3) was used to study the sequences from 31 to 110. Hydrophobic amino acids (Phe, Tyr, Ile, Leu, Val, Met, Ala, Trp, His, and Thr), defined as those with $\Delta G$ values >0.4 kcal/mol to transfer the amino acid side chain from water to ethanol (22) were used to search for heptad repeat sequences with the possibility to form amphipathic helixes (hydrophobic amino acids in *a* and *d* positions) with the program PSEARCH PCGene (Intelligenetics, Geneva, Switzerland) (5). Alignment of Pro, Gly, or hydrophobic amino acids was performed manually. Sequences from eight pG of VHSV were obtained from GenBank™ accession numbers X59148 and X66134 and six unpublished sequences.[2]

*Peptide and Pepscan Synthesis*—Peptides p2 ($^{82}$IIHLPLSVTSVSAVASGHYLHRVTYRVT$^{109}$), p3 ($^{110}$CSTSFFGGQTIEK$^{122}$), p4 ($^{123}$TILEAKLSRQEATDEASKDHEY$^{144}$), and p9 ($^{58}$RPAQLRCPHEFEDINKGLVSVPT$^{80}$) (Fig. 1*B*) were synthesized by CLONTECH (Palo Alto, California). The numbers correspond to the amino-terminal positions in the pG from VHSV 07.71 (23), including the signal peptide. The biotinylated peptide of 28 amino acids derived from fragment 11 was chosen to decrease self-aggregation (biotin-$^{68}$FEDINKGLVSVPTRIIMLPLSVTSVSAV$^{95}$). The amino-terminal poly(H) peptide tail added by the pRSETa plasmid to cloned fragment 11 (MGGSHHHHHHGMASMTGGQQMGRDLYDDDDKD) was also synthesized to be used as a control, since attempts to remove it from fragment 11 with enterokinase were unsuccessful. Synthesis of a series of 15-mer peptides overlapping 5 amino acids covering all of the cDNA-derived protein sequence of the pG (Pepscan) (23) of VHSV 07.71 was performed by Chiron (Chiron, Mimotopes, Victoria, Australia).

*VHSV Concentration and VHSV Infection Assay*—The VHSV 07.71 (24) was used to obtain RNA to clone fragment 11, to concentrate VHSV, and to purify pG. The VHSV was grown in epithelial papullosum cyprini (EPC) cells and concentrated by polyethyleneglycol to about 70% purity as described before (25). The VHSV assay was similar to the microneutralization assay described before (26). Briefly, about 100 VHSV foci-forming units/well of a 96-well plate were added to EPC cell monolayers at 14 °C. After 1 day, infected foci were stained with 2C9 anti-N VHSV mAb, peroxidase-labeled anti-mouse IgG, and diaminobenzidene (DAB) and then counted.

*Cloning of Fragment 11*—The sequence corresponding to 56–110 of the pG of VHSV 07.71 (23) was amplified by the polymerase chain reaction from cDNA made from its isolated RNA (Fig. 1*B*). The sequence was then cloned into a pRSETA plasmid (Invitrogen, San Diego, CA), used to transform the *Escherichia coli* DH5α strain to select a positive clone, and then the construction was transferred to *E. coli* BL21 DE3 for expression as described before (27).[3] The nucleotide sequences corresponding to pG sequences 56–110 were present in the recombinant plasmid as demonstrated by DNA sequencing of the insert in both directions (not shown). For expression, isopropyl-1-thio-β-D-galactopyranoside was added following the manufacturer's instructions, and the bacterial lysates in lysis buffer (20 mM $Na_2HPO_4$, 0.5 M NaCl, 6 M guanidine HCl, pH 7.8) were eluted from a nickel affinity column (ProBond™, Invitrogen) at pH 4.

Interaction of fragment 11 with itself was detected by its tendency to precipitate out of solution when dialyzed against 0.15 M phosphate-citrate, pH 7.6 (7). The highest concentrations of 50, 180, 260, or more than 1000 μg of dissolved fragment 11/ml were obtained by using pH values of 7.6, 6, 5.6, or 4, respectively. Only a small percentage of the aggregates were disulfide-bridged, as shown by densitometry of the Coomassie-stained bands of fragment 11 separated by 15% polyacrylamide gel electrophoresis in the presence of SDS and in the absence of β-mercaptoethanol. When kept at pH 4 before the polyacrylamide gel electrophoresis, 94.2% of fragment 11 was in the monomeric form, the rest being dimers (2.7%), trimers (1.9%), and higher molecular weight aggregates that did not penetrate the polyacrylamide gel (1.1%). Similar compositions were estimated when aggregates were formed during 2 h at pH 6 or 7.6 before performing polyacrylamide gel electrophoresis. On the contrary, only one band at about 10 kDa was obtained by polyacrylamide gel electrophoresis in the presence of SDS and β-mercaptoethanol, other higher molecular weight bands being undetectable at the highest concentrations electrophoresed (50 μg of fragment 11/well, $n = 12$). Since only one peak at $A_{280}$ and at the same position was obtained after fragment 11 was separated by Sephadex chromatography in buffers at pH 4 in the absence or in the presence of 0.14 M β-mercaptoethanol, Sephadex G-100 chromatography at pH 4 was used to purify fragment 11 from other higher molecular weight components.

*Induction of Anti-fragment 11, Anti-p2, Anti-p3, Anti-p4, and Anti-pG Abs in Mouse Ascites*—Female BALB/c mice in groups of three were each immunized by injection with 20 μg of fragment 11, p2, p3, p4, or purified pG (29) in Freund's complete adjuvant and then by four monthly similar peptide injections in Freund's incomplete adjuvant. To obtain pooled diluted ascites containing the Abs, the immunized mice were intraperitoneally injected each with 0.5–2 × $10^6$ viable myeloma X63/Ag8653 cells as described before (30).

*Enzyme-linked Immunosorbent Assays*—Confirmation of fragment 11 identity was performed by using polyclonal Abs (15) obtained in mice ascites against concanavalin A affinity-purified pG from VHSV (29). Wells (Polysorp, Nunc) were coated with serial dilutions of fragment 11 or other proteins in 100 μl of water and allowed to dry overnight at 37 °C. The coated plates were washed with dilution buffer before use. Then anti-G Abs (5 μg/ml) in dilution buffer (0.5% bovine serum albumin, 0.3% rabbit serum, 0.1% Tween 20, 0.01% merthiolate, 0.005% phenol red in phosphate-buffered saline) were added to the plates and incubated during 1 h at room temperature.

Recognition of segments in the pG by the corresponding Abs was carried out in plates coated with VHSV (0.5 or 1.5 μg of viral protein/ml) in 0.1 M citrate phosphate buffer at pH 7.6 and 6. Mice ascites containing Abs to p2, p3, p4, and fragment 11 were diluted 100–300-fold (to give a maximum absorbance of 1.5–2 units) in dilution buffer at different pH values and incubated for 1 h. Backgrounds, in wells coated with bovine serum albumin and incubated with the same antibodies at the same dilutions or in a well coated with VHSV and incubated with irrelevant ascitic fluid at the same dilutions ranged between 0.1 and 0.6 absorbance units. Backgrounds were subtracted for all of the data. The relative absorbances were calculated according to the following formula: absorbance at pH 5.6/absorbance at pH 7.6 × 100.

Recognition of solid-phase VHSV plus fragment 11 mixtures by anti-G mAbs was performed by coating the wells to dryness with serial dilutions of fragment 11 + VHSV in 100 μl of volume. Then anti-G mAbs of known target epitope in dilution buffer at different pH values were added to the wells and incubated for 1 h.

Recognition of lineal epitopes by fragment 11 was performed by using Pepscan peptides from the pG and a biotinylated peptide from fragment 11. The Pepscan peptides diluted in 5 mM HEPES, pH 7.6, were dried in 96-well polystyrene plates (Dynatech, Plochingen, Germany) by using 100 μl/well at a final concentration of about 3 nmol/well. The biotinylated peptide (10 μg/ml) was diluted in 150 mM citrate-phosphate buffer at pH 7.6 or 5.6, pipetted into the plates (100 μl/well), and incubated with the Pepscan-coated plates during 1 h. To detect the biotinylated peptide, 200-fold diluted streptavidin-peroxidase (Nordic, The Netherlands) was added to the wells.

In all cases mentioned above, after washing, the mice Abs were detected with 100 μl of 300-fold diluted horseradish peroxidase-conjugated goat anti-mouse Ab (Sigma). The color reaction was developed by adding 1 mg/ml *o*-phenylenediamine in 150 mM citrate buffer containing 3 mM $H_2O_2$. Optical density was measured at 492–620 nm (dual wave length) in an enzyme-linked immunosorbent assay reader as indicated before (31).

[2] A. Benmansour, unpublished results.

[3] A. Rocha, M. Fernandez-Alonso, V. Mas, L. Perez, A. Estepa, and J. M. Coll, submitted for publication.

*Solid-phase Phospholipid-binding Assays*—Screening of phospholipid binding in the pG Pepscan peptides was made by using labeled anionic and nonionic phospholipids with the same carbon backbone to increase specificity. The labeled phospholipids used, 1 Ci/mmol, phosphatidyl-[2-$^3$H]inositol 4,5-bisphosphate (PIPP) and phosphatidyl [2-$^3$H]inositol (PI) (Amersham Pharmacia Biotech), were dissolved in organic solvents, dried into glass tubes, mixed with 150 mM phosphate-citrate buffer at pH 5.6 (7), and then sonicated at 4 °C for three 1-min periods. Labeled phospholipids in phosphate-citrate pH 5.6 buffer (100 μl/well) were added to the 96-well Pepscan peptide-coated plates. After 4 h of incubation at 4 °C, the plates were washed three times with distilled water and incubated with 100 μl/well 2% SDS 50 mM ethylenediamine, pH 12, at 60 °C for 30 min. The extracts were transferred to 96-well polyethylene terephthalate plates (Amersham Pharmacia Biotech), 100 μl/well Hiload scintillation liquid (Amersham Pharmacia Biotech) was added and mixed, and plates were counted on a 1450-Microbeta scintillation counter (Wallac, Turku, Finland; Amersham Pharmacia Biotech), as described before (15).

*Lipid Vesicle Preparation*—A phospholipid film was obtained upon overnight drying of a chloroform solution under vacuum in a glass tube. The phospholipids (Avanti Polar Lipids, Alabaster, AL) were suspended at 1 mg/ml in 100 mM NaCl, 5 mM MES, 5 mM sodium citrate, 5 mM Tris, 1 mM EDTA (medium buffer) adjusted to the desired pH and incubated for 1 h at 37 °C and vortexed vigorously and adjusted to 0.14 mM final concentration. This suspension was extruded by 19 cycles in a Liposo-Fast™ Basic extrusion apparatus with 100-nm polycarbonate filters (Avestin Inc.).

*Vesicle Aggregation Assay*—We used an assay based in the increase in the size of phospholipid vesicles quantified by optical density, since it has been used before as an indicator of vesicle fusion (32). The assay was performed as described before (1). Fragment 11 and p2 were added from a stock solution of 5 mg/ml in 20 mM MES at pH 5.6 to phospholipid vesicle suspensions in 1 ml of medium buffer at the desired pH.

*Infrared Measurements*—The measurements were performed as described before (1) in D2O buffer containing 10 mM HEPES, pH 7.0, 130 mM KCl, and 20 mM NaCl.

*Circular Dichroism*—The measurements were performed as described before (1). Aliquots of fragment 11 or p9 peptide from a solution at 5 mg/ml in trifluoroethanol were added to medium buffer (100 mM NaCl, 5 mM Tris, 5 mM citrate, 5 mM MES, 1 mM EDTA) at the desired pH to give a final concentration of the peptide of 32.5 μM. The mixtures of fragment 11 or p9 and PS were incubated for 1 h at 37 °C and then sonicated to disrupt the large aggregates that could cause light scattering artifacts.

*PS Detection in the Plasma Membrane of EPC Cells Exposed to Fragment 11*—To estimate PS exposure induced by fragment 11, we chose EPC cell monolayers as a model of biological membranes with asymmetrical distribution of PS in the inner leaflet of the plasma membrane. Because dead cells expose PS in the outer leaflet of the plasma membrane, those were detected by staining with propidium iodide (PrIo). EPC cells expressing PS in the plasma membrane outer leaflet were identified as those intact cells binding fluorescein (FITC)-labeled annexin V (CLONTECH) and excluding PrIo after a 60-min incubation with peptides in RPMI 1640 (without bicarbonate) buffered with 20 mM HEPES and 20 mM MES at pH 6 and at 14 °C. A lower pH was not used to avoid excessive damage and/or detachment of the monolayer cells during the exposure at that pH. The EPC cells were grown in 24-well plates, stained with 1 μl of FITC-labeled annexin V in 100 μl of cell culture medium for 15 min, detached with 10 mM EDTA in PBS, and analyzed on a Becton Dickinson flow cytometer. The results were analyzed with the Lysis software (Becton Dickinson, Franklin Lakes, NJ). Annexin V-positive, PrIo-negative cells were determined by setting regions to separate those from PrIo-positive (dead cells) and annexin V-negative cells, by following the manufacturer's instructions. The percentage of cells positive for PS appearance was determined from the cells staining greater than 95% of the control population threshold. PrIo-positive dead cells were lower than 8% in all cases.

*Low pH-induced Fusion Assays by Fragment 11 or pG-transfected Cells*—To assay for fragment 11-induced cell spreading and fusion from without, the assay was performed in 24-well plates under similar conditions to those described before (19). Fragment 11 was added in fusion medium, RPMI 1640 (without bicarbonate) buffered with 20 mM HEPES, 20 mM MES (Sigma) at pH 6 to EPC monolayers for 30 min at 14 °C. To assay for cell spreading, the cell monolayers were fixed after this step. To assay for fusion, the cultures were then washed with fusion medium at pH 7.6 and incubated during 2 h more at 14 °C with fusion medium at pH 7.6.

To assay for pG-induced fusion from within, EPC cells in 24-well plates (about 100,000 cells/well) were transfected with 0.6 μg of the plasmid G3-pcDNAI/Amp complexed with 2 μl of Fugene in 100 μl of volume following the methods described before (33, 34). Abs were serially diluted in fusion medium at pH 6 (optimal fusion pH) (19) and incubated overnight at 4 °C. The next day, the EPC plates were washed, and the serial dilutions of Abs were pipetted into the EPC wells. After 30 min of incubation, the cultures were washed with fusion medium at pH 7.6 and incubated for 2 h at 14 °C with fusion medium at pH 7.6.

In both assays mentioned above, after removal of the fusion medium, the EPC cell monolayers were fixed in 1% glutaraldehyde for 10 min, dried, and stained with Giemsa. The spread cells (cell surface of spread cells, 2–3-fold the control EPC cell surface) were counted among 400 cells. Results were expressed by the following formula: number of spread cells/number of total cells × 100. The number of nuclei in syncytia of three or more nuclei per syncytium were counted among 400 nuclei/well. Results were expressed as the percentage of nuclei in syncytia by the following formula: number of nuclei in syncytia/total number of nuclei × 100.

## RESULTS

*Selection of pG Segments around the p2 Phospholipid-binding Domain of VHSV*—A series of segments of the pG from the positions 56–144 that surround the phospholipid-binding domain (p2, sequence 82–109) were used to investigate which region(s) might be involved in membrane perturbation events (Fig. 1*B*). The segments were then synthesized as peptides p9 (sequence 58–80), p2 (sequence 82–109), p3 (sequence 110–122), and p4 (sequence 123–144). Peptide p9 contained 23 amino acids from position 56 to the beginning of p2. Following p2, p3 contained a sequence of 12 amino acids, 11 of which were totally conserved among cold water fish rhabdoviruses (VHSV, infectious hematopoietic necrosis virus, and hirame rhabdovirus) (3). Peptide p4 was from the end of p3 to the beginning of the putative fusion peptide (sequence 142–159). It contained many hydrophilic amino acids and one of the sites (K140) mutated in neutralization-resistant VHSV mutants of mAb C10 (21, 35).

Fragment 11 (sequence 56–110) containing the p9 + p2 sequences and five heptad repeats (sequence 68–99) (Fig. 1*A*) was obtained as a recombinant fragment. The segment corresponding to fragment 11 in the pG is flanked by disulfide bridges $Cys^{64}$–$Cys^{315}$ and $Cys^{110}$–$Cys^{152}$ (4), bringing together the phospholipid-binding and putative fusion domains (Fig. 1, *A* and *B*).

*Binding of Labeled Phospholipid Vesicles to Solid-phase Peptides from a Pepscan of pG*—To investigate p9, p2, p3, p4, or fragment 11 binding of anionic phospholipids, solid phases made of each of the five amino acids overlapping 15-mer peptides covering the whole sequence of pG (Pepscan) were used. Labeled phospholipids were PIPP as an anionic phospholipid and PI as the best control for PIPP, since it has less charge than and the same carbon backbone as its bisphosphate derivative. Maximal PIPP binding (10–14-fold the background level) was found by peptides covering the sequence 83–113 (corresponding to p2). Lower PIPP binding (4–6-fold the background level) was found by peptides covering the sequence 109–133 (including p3) and by peptides covering the sequence 149–173 (including most of the putative fusion peptide) (Fig. 2*A*). However, Pepscan peptides covering the sequence of p9 and p4 did not show PIPP binding above background. Other peptides from the Pepscan also showed significant PIPP binding at other positions outside the studied region (*e.g.* those at around sequence 230). Very low binding was obtained for all peptides from the Pepscan when labeled PI was used (Fig. 2*B*).

*Aggregation of Phospholipid Vesicles by p2 and Surrounding Segments*—Concentrations from 1 to 100 μg/ml peptides were added in solution to 0.14 mM phospholipid vesicles of PS, phosphatidic acid, phosphatidylglycerol, or phosphatidylcholine at pH 7.6 and 5.6. The interactions of fragment 11 or p2 with

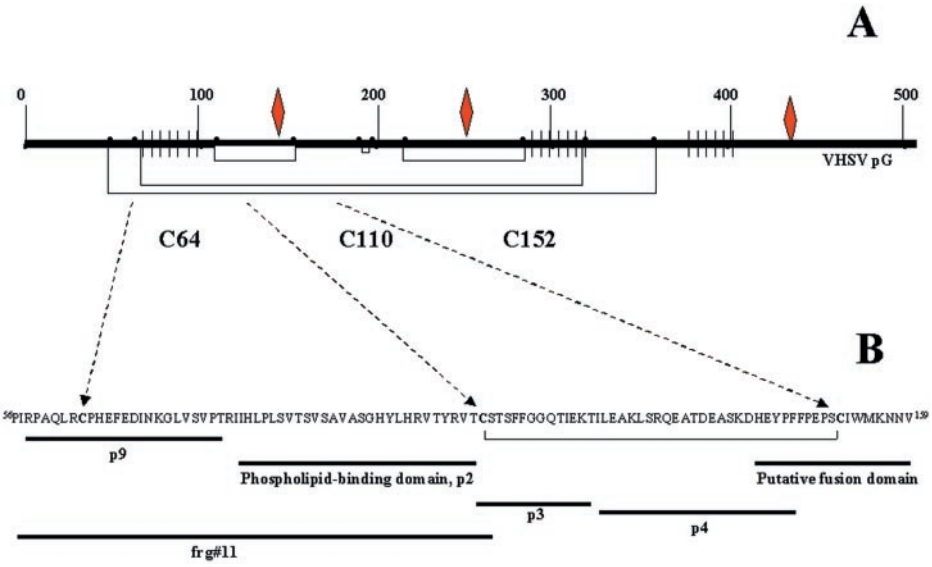


FIG. 1. **Disulfide bridges, heptad repeats, and neutralizing mAb-resistant mutant positions of the pG of VHSV (*A*) and location of p9, p2, p3, p4, and fragment 11 (*frg#11*) sequences in the pG (*B*).** *A*, *thick line*, sequence of pG from VHSV; ●, cysteines connected by *horizontal lines* representing its pairing by disulfide bridges (4). Cysteines around the phospholipid-binding domain are $Cys^{64}$ ($C_I$), $Cys^{110}$ ($C_{III}$), and $Cys^{152}$ ($C_{IV}$) (I, II, and III according to Walker (3). *Vertical lines*, hydrophobic heptad repeat regions according to Coll (5). ♦, C10 mAb-resistant mutants mapping at positions 140 and 433 and 2F1A12 mAb-resistant mutants mapping at position 253. *B*, sequence and location of p9 (sequence 58–80), phospholipid-binding domain p2 (sequence 82–109), cold water fish rhabdovirus conserved sequence p3 (sequence 110–122), highly hydrophilic loop p4 (sequence 123–144), heptad repeat domain fragment 11 (sequence 56–110), and putative fusion peptide (sequence 142–159). Cysteines 64, 110, and 152 are in *boldface type*, and $Cys^{110}$ is bridged to $Cys^{152}$ (*horizontal line*).

anionic phospholipid vesicles showed 1.5-fold higher OD values at pH 5.6 than at pH 7.6 ($n = 3$), PS being the phospholipid showing the greatest anionic phospholipid vesicle aggregation (Fig. 2*C* and data not shown). Fragment 11 aggregated PS vesicles with 5-fold more efficacy when compared with p2 in a molar basis. In the presence of phosphatidylcholine, however, the increase in optical density was almost negligible even at pH 5.6. Peptide p9, p3, p4, or poly(H) did not induced any increase in the optical density at 360 nm in the presence of any of the phospholipids mentioned above (results not shown).

*Induction of Cell Spreading and Syncytia by p2 and Surrounding Segments*—When fragment 11 or p2 was added to EPC cell monolayers at pH 6, there was a 2–3-fold increase in the cell surface (cell spreading) in some of the cells (Fig. 3*A*). Thus, at pH 6 the addition of fusion medium, p2 (200 μg/ml) or fragment 11 (200 μg/ml) induced cell spreadings of 3.4 ± 0.2, 33.0 ± 1.0, or 36.7 ± 2.4% of the EPC cells, respectively ($n = 2$). The addition of p9, p3, p4, or poly(H) at pH 6 or fragment 11 at pH 7.6 to the EPC cell monolayers produced no detectable effects in cell spreading (not shown).

In the same experiments, syncytia of 3–6 nuclei also appeared but only in the presence of fragment 11 at pH 6 (Fig. 3*C*). The percentage of nuclei inside syncytia increased from 5 to 10% of the total number of nuclei when adding 50–200 μg of fragment 11/ml to EPC cell monolayers (Fig. 3*E*). The addition of p2, p3, p4, or poly(H) to the EPC cell monolayers did not cause numbers of syncytia higher than 2% (Fig. 3*E* and results not shown). Since ~10 μg of VHSV (containing about 1 μg of pG)/ml were required to obtain a similar highest number of nuclei in syncytia (not shown), fragment 11 was ~200-fold less active than pG in inducing fusion in cell monolayers. However, this fragment 11 concentration requirement for fusion is, most probably, an overestimation because of the tendency of fragment 11 to aggregate, as shown by the presence of visible microscopic aggregates covering the cell monolayers. Aggregates such as those are unlikely to cause the observable effects, that must be attributed to the fragment 11 molecules that remain in solution. Since only 15–30% of fragment 11 remains in solution in phosphate-citrate at pH 6, the concentration of the fusion-active soluble fragment 11 molecules that caused fusion at that pH are probably 3–6-fold lower than the concentration added. The percentage of cell to cell fusion was also dependent on the initial EPC cell concentrations. The higher the concentration was, the higher the percentage of nuclei in syncytia. However, concentrations of >300,000 cells/well resulted in such high numbers of nuclei in syncytia that they could not be quantitated.

*Induction of PS Exposure in the Plasma Membrane by p2 and Surrounding Segments*—Membrane fluorescence to FITC-labeled annexin was observed in some of the EPC cells exposed to 20 μg/ml fragment 11 at pH 6 (Fig. 4, *A* and *B*). To quantitate the translocation of PS to the other side of a biological membrane, we used the plasma membrane of EPC cells as a model and FITC-labeled annexin-binding to the cell surface of living cells as an estimation of PS exposure. An increase in the number of FITC-labeled annexin cells could be detected among the viable (PrIo-negative) cells after EPC cell monolayers were treated at pH 6 with increasing concentrations of fragment 11 (Fig. 4*C*) up to 400 μg/ml (not shown). The addition of p9, p2, p3, p4, or poly(H) was unable to induce such a significant number of annexin V-positive, PrIo-negative EPC cells in parallel experiments at those concentrations (Fig. 4*C* and data not shown).

*Low pH- and Phospholipid-dependent Conformations of Fragment 11*—Since fragment 11 appeared to be the most important segment in relation to fusion of those studied, the possible pH-dependent conformations suggested by the pH-dependent reversible aggregation of fragment 11 (see "Materials and Methods") were measured by IR and CD spectra at different pH values.

From neutral to low pH, the band decomposition of the original amide spectra showed an increase in the band at 1633–1637 nm, corresponding to an increase in β-sheet content from 5.8 ± 1.2 to 25.4 ± 2.7% and other minor changes (not shown). The CD spectrum of fragment 11 at pH 5.6 shows the presence of 34.4% of β-sheet conformation, similar to the data obtained by the IR spectra. However, in the presence of PS vesicles, the β-sheet conformation of fragment 11 increased to

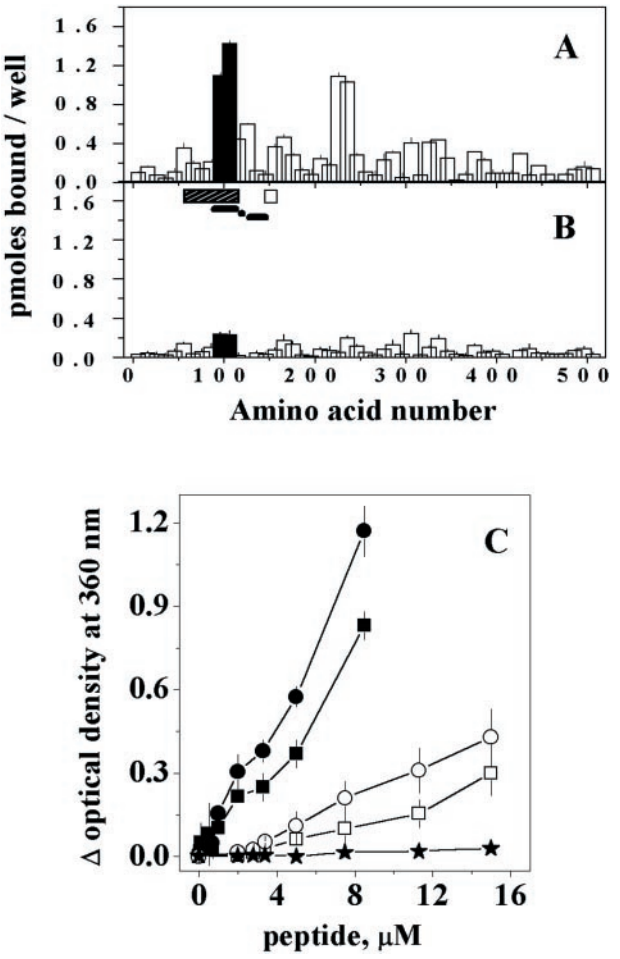


FIG. 2. **Binding of labeled phosphatidylinositol bisphosphate (*A*) and phosphatidylinositol (*B*) vesicles to solid-phase 15-mer Pepscan pG peptides and increase in the optical density induced by the addition of fragment 11 or p2 to phosphatidylserine vesicles at pH 7.6 and 5.6 (*C*).** *A*, sonicated vesicles containing 10 pmol/well labeled PIPP (*A*) or PI (*B*) in 0.15 M phosphate-citrate at pH 5.6 were dispensed in solid-phase plates coated with about 3 nmol/well 15-mer Pepscan peptides. After incubating and washing, the wells were counted, and results were calculated and expressed in pmol of phospholipid bound/well. Averages and S.D. values from duplicates are represented. Similar results were obtained at pH 7.6. ■, highest PIPP-binding peptides covering the sequence 83–113 corresponding to the p2 part of fragment 11 (sequence 56–110) (*horizontal hatched bar*). *Black horizontal bars*, location of p2, p3, and p4, respectively, from *left* to *right*. *Open horizontal bar*, location of the putative fusion domain. *C*, different concentrations of fragment 11 or of p2 from 5 mg/ml solutions in 20 mM MES, pH 5.6, were added to 0.14 mM PS vesicles in medium buffer at the final pH. The increment of optical density at 360 nm was measured after incubating the mixtures during 1 h at 37 °C and calculated by the following formula: optical density in the presence of PS − optical density in the absence of PS. ●, fragment 11 + PS at pH 5.6; ■, fragment 11 + PS at pH 7.6; ○, p2 + PS at pH 5.6; □, p2 + PS at pH 5.6; *, poly(H) peptide + PS at pH 5.6 or 20 mM MES + PS at pH 5.6.

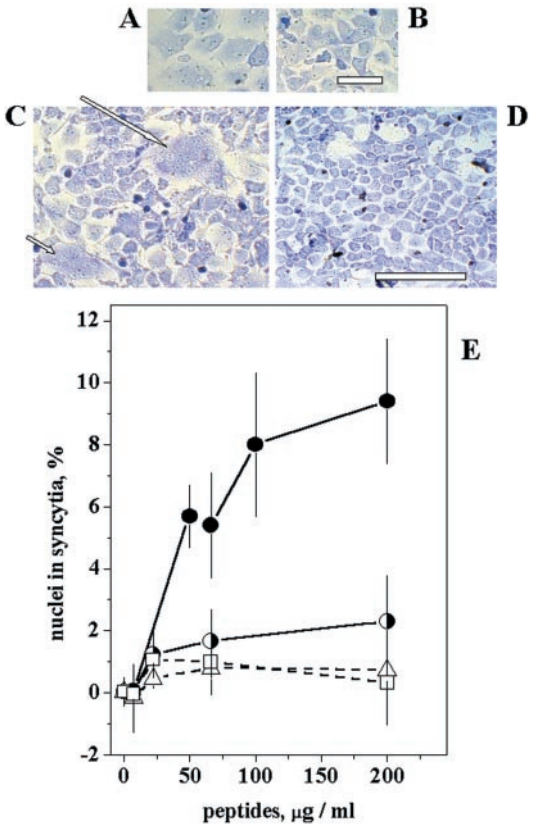


FIG. 3. **Microphotographs of cell spreading (*A* and *B*) and syncytia formation (*C* and *D*) in EPC cell monolayers after the addition of fragment 11 and dependence of the percentage of nuclei in syncytia with the concentration of fragment 11 (*E*).** To make the microphotographs, EPC cell monolayers were treated with 20 μg of fragment 11/ml during 30 min at pH 6 and 14 °C. Then the monolayers were fixed and stained with Giemsa. *A*, fragment 11-treated EPC cell monolayers showing cell spreading with respect to EPC cell monolayers treated under the same conditions but in the absence of fragment 11 (control, *B*). The *horizontal bar* is 30 μm. *C*, fragment 11-treated monolayers showing syncytia (*arrows*). *D*, control EPC cell monolayers. *Horizontal bar*, 100 μm. Peptides were added to EPC cell monolayers grown in 24-well plates and incubated for 30 min at pH 6 and 14 °C. Then the cultures were washed with cell culture medium at pH 7.6 and incubated 2 h more. To estimate induced fusion, the monolayers were fixed and stained with Giemsa. The numbers of nuclei in syncytia of three or more nuclei were then counted among 400 nuclei/well. Results were expressed as the percentage of nuclei in syncytia by the following formula: number of nuclei in syncytia/total number of nuclei × 100. Average and S.D. from three experiments are represented. ●, fragment 11; ◑, p2; △, p3; □, p4.

84.4% to become the major component (Fig. 5 and Table I), and at the same time the β turns decreased from 28.2 to 1.7%. Increasing the phospholipid/peptide molar ratio from 11 to 40:1 did not modify the CD spectrum any further, but at the intermediate phospholipid/fragment 11 molar ratio of 20:1, and despite the low pH, aggregates formed, which made it impossible to record any spectrum. Sonication was not capable of disrupting these aggregates, most probably formed as a result of neutralization of the electrostatic charges. The addition of PS to poly(H) did not induce any changes in its CD spectra (not shown), and the addition of phosphatidylcholine to fragment 11 produced only minor disturbances on the CD spectra of fragment 11 (not shown). At pH 7.6, the CD spectra could not be obtained because of aggregation of fragment 11 or of fragment 11 plus PS.

*Inhibition of Cell-to-Cell Fusion of pG Gene-transfected Cells by Antibodies to p2 and Surrounding Segments*—Because, in general, studies with peptides in isolation (such as those mentioned above) are difficult to interpret and sometimes the results bear little relation to what the corresponding sequences do in the context of the native protein, attempts were made to show the relevance of fragment 11 to VHSV fusion.

Because EPC cell monolayers transfected with a plasmid coding for the pG of VHSV caused about 25% of nuclei to be in syncytia when incubated at pH 6, an assay was designed to estimate the fusion in the presence of Abs to the selected segments around p2. To best interpret those experiments, binding of anti-peptide Abs to solid-phase VHSV pG were first studied at neutral (pH 7.6) and at fusion pH (pH 6). Thus, all of the anti-peptide Abs recognized each of their target pG segments in VHSV at both pH values. However, at low pH, Abs to

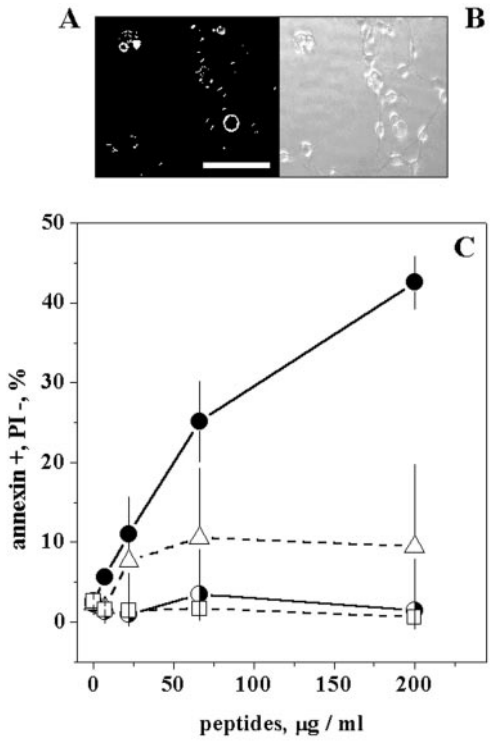


FIG. 4. **Microphotographs of FITC-labeled annexin V-stained cell monolayer after exposure to fragment 11 under fluorescence (*A*) or under phase-contrast (*B*) microscopy and dependence of the percentage of FITC-labeled annexin V cells (*C*) with the concentration of fragment 11 as estimated by cytofluorometry.** To make the microphotographs, EPC cell monolayers were treated with 20 $\mu$g of fragment 11/ml for 60 min at pH 6 and 14 °C and then stained with FITC-labeled annexin V. *Bar*, about 100 $\mu$m (*A* and *B*). To quantitatively estimate PS exposure (*C*), the EPC cell monolayers were stained with FITC-labeled annexin V and PrIo, detached with 10 mM EDTA in PBS, and analyzed by flow cytometry. Percentage of cells positive for PS and negative for PrIo was determined from the cells staining greater than 95% of the control (fragment 11 nonexposed) population thresholds. ○, fragment 11; ◑, p2; △, p3; □, p4.

fragment 11 or p2 recognized their pG segments with 5- or 2-fold higher absorbance, respectively, than Abs to p3 or p4. Under the conditions employed, the disulfide-dependent neutralizing mAbs C10 and 2F1A12 bound to solid-phase pG VHSV similarly whether the binding was carried out at pH 7.6 or at 6 (not shown). Binding of each of the Abs to its corresponding solid-phase peptides was also similar whether carried out at pH 7.6 or 6 (not shown). Under the same conditions at which anti-peptide Abs bound to the pG in solid-phase VHSV, Abs to fragment 11, p2, and p4 reduced the number of nuclei in syncytia when compared with Abs to p3 (Fig. 6) or irrelevant mAbs (mAb anti-N 2C9, to the nucleoprotein of VHSV) (not shown). In parallel experiments, neutralizing mAbs C10 and 2F1A12 and polyclonal anti-pG Abs also inhibited syncytia formation (not shown).

## DISCUSSION

*Participation of the Fragment 11/p2 in VHSV Fusion*—Of all of the selected segments p9, p2, p3, p4, and fragment 11 (p9 + p2), fragment 11 showed the highest anionic phospholipid aggregation specific activity and was the only one to induce noninfected cell-to-cell fusion and to translocate PS from the inner to the outer leaflet of the plasma membrane. Although PS translocation might be expected from a peptide interacting and destabilizing a membrane, to our knowledge it has not been described before for any viral derived peptide. Fragment 11 contained 84.4% $\beta$-sheet structure at the low pH required for most of its phospholipid-related activities.

Anti-fragment 11 inhibition of pG-transfected cell-to-cell fusion at low pH confirmed the implication of the fragment 11 domain in fusion. Fragment 11 showed different reversible pH-dependent conformations as shown by dramatic and reversible changes in its solubility and by changes in its IR or CD spectra (from 5.8 to 25.4–34.4% $\beta$-sheet content from neutral to low pH). It is likely that similar conformational changes in fragment 11 would contribute to its pH-dependent exposure at the surface of pG during fusion as suggested by its increased recognition and inhibition of fusion at low pH with anti-fragment 11 and anti-p2 Abs. Exposure of a previously buried region at the surface of pG at the low pH of fusion had been demonstrated before for rabies virus (8) and for vesicular stomatitis virus (36). Although the Abs mentioned earlier might also inhibit fusion by steric hindrance, the anti-fragment 11 and anti-p2 inhibition of fusion, together with all the other results of this work, strengthens the participation of fragment 11 and of p2 in fusion.

Although the addition of p2 at low pH to an EPC monolayer spreads the cells (most probably due to its insertion into the membrane) (1), only fragment 11 induced both spreading (Fig. 3*A*) and cell-to-cell fusion of the cells (Fig. 3*C*). However, fragment 11 was about 200-fold less efficient as pG in inducing cell-to-cell fusion. The estimated fragment 11 fusion-specific activity, however, can be at least 3–6-fold higher due to the presence of inert aggregates in the preparations of fragment 11 at the pH of fusion. Nevertheless, the results suggest that VHSV fusion requires not only the fragment 11 domain but also of some other domain(s) of pG, similar to what occurs in vesicular stomatitis virus, in which efficient viral cell fusion required not only fusion (12) but also carboxyl-terminal (10) and transmembrane (37) domains.

Since one molecule of p2 binds 15–17 molecules of anionic phospholipids (1) and a ~1:20 molar ratio was required to form aggregates between fragment 11 and anionic phospholipids, we can speculate about the number of molecules participating in the fusion process involving pG trimers. Thus, by assuming a similar situation in VHSV as in rabies virus fusion, where six pG trimers form the minimal fusion complex (8), the penetration of p2 in the membranes would cause a local increase of both p2 (6 × 3 p2 domains per fusion complex) and anionic phospholipids (270–360 anionic phospholipid molecules/fusion complex). The translocation of all of these molecules of anionic phospholipids from the inner to the outer leaflet of the membrane by the fragment 11 domains of a minimal fusion complex would cause a high local destabilization in most membranes, making them easier to fuse, as occurs in pH-sensitive liposomes (28).

*Participation of p9, p3, and p4 in VHSV Fusion*—Given the low affinity of fragment 11 for phosphatidylcholine, an external membrane phospholipid, the initial interaction of fragment 11 with the cellular membranes, contrary to what occurs with the anionic phospholipid vesicle models, must involve some protein-protein interactions. Most probably, those interactions are p9-dependent, since in fragment 11 only the p9 part does not bind phospholipids (Fig. 2 and CD spectra) and is free to interact with other peptide(s), at least after p2 has penetrated into the membrane. Also the covalent union between p9 and p2 must play an important part in the aggregation of fragment 11 at neutral pH, since there is no aggregation of the isolated p9, p2, or p9 + p2 parts of fragment 11 (not shown). Furthermore, aggregated PS vesicles were obtained with fragment 11 with 5-fold more molar specific activity than with p2, suggesting that some of the observed differences in PS aggregation by fragment 11 might be due to p9 interactions. On the other hand, it is difficult to explain how fragment 11 would undergo

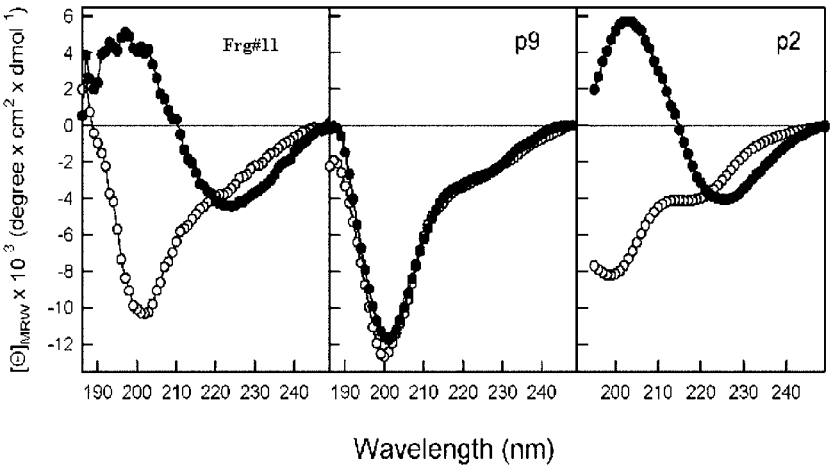


FIG. 5. **CD spectra of fragment 11 (*frg#11*), p9, and p2 alone or incubated with phosphatidylserine vesicles.** Fragment 11, p9, and p2 at 100 $\mu$g/ml in medium buffer at pH 5.6 were incubated in the absence (○) or in the presence (●) of PS vesicles at a lipid/peptide molar ratio of 11:1 (similar results were obtained at a ratio of 40:1). Sonication was used to disrupt the small amount of aggregates formed in order to eliminate light scattering. The results obtained at different path lengths were similar, so there were no light scattering effects on the registered spectra. The distribution of secondary calculated structure is shown in Table I. Values for p2 have been included here for comparison (1).

TABLE I
*Secondary structure of fragment 11 and its two peptide components p9 and p2 from CD data at low pH*

Data are expressed as percentages. Values for p2 were published before and are included here for comparison (1).

| | Fragment 11 (56–110) | p9 (58–80) | p2 (82–109) |
|---|---|---|---|
| Peptide alone | | | |
| $\beta$-Sheet | 35.3 | 31.8 | 28 |
| Nonordered | 36.5 | 34.7 | 31 |
| $\beta$-Turn | 28.2 | 33.5 | 43 |
| Peptide + PS | | | |
| $\beta$-Sheet | 84.4 | 32.2 | 91 |
| Nonordered | 13.9 | 34.2 | 8 |
| $\beta$-Turn | 1.7 | 33.6 | 1 |

a reverse orientation in the membrane to cause PS translocation in the absence of additional pG sequences to aid in the process without the participation of p9. Therefore, the results suggest that p9 adds some peptide-peptide interactions to fragment 11, underline the importance of p9, and make it a good candidate to bring cellular membranes closer to each other before fusion.

The electrostatic attraction between the positively charged amino acids of p2 and the negatively charged phospholipids in the cytosol-facing monolayer of the endosome membrane could provoke the extension of the $\beta$-sheet structure of fragment 11 (CD of fragment 11 in the presence of anionic phospholipids). Because p9 (no changes in CD spectra and negative Pepscan PIPP binding) or p4 (high hydrophilicity and negative Pepscan PIPP binding) did not interact with anionic phospholipids, only p2 (1), p3 (noncharged amino acids and some Pepscan PIPP binding), and the putative fusion domain (some Pepscan PIPP binding) might be favored to get inside the hydrophobic part of the membranes. Inhibition of the penetration of the membrane by fragment 11/p2 could thus explain the inhibition of syncytia formation by anti-fragment 11/p2 Abs, whereas inhibition of p4 conformational changes required for fusion could explain the inhibition by anti-p4 (Fig. 6).

In VHSV, as in other rhabdoviruses and contrary to other enveloped viruses, the putative fusion domain that inserts itself into the membrane remains uncleaved during fusion, is not hydrophobic, and contains a cysteine, and the low pH-induced conformational changes accompanying fusion are reversible. The reversible insertion of an internal fusion domain into a membrane bilayer would require at least one bending or a U structure. Since the low pH reversible conformational changes in fragment 11 described in this work correlate with the reversible low pH conformational changes of pG required for fusion in rhabdoviruses, the fragment 11 domain fulfills the

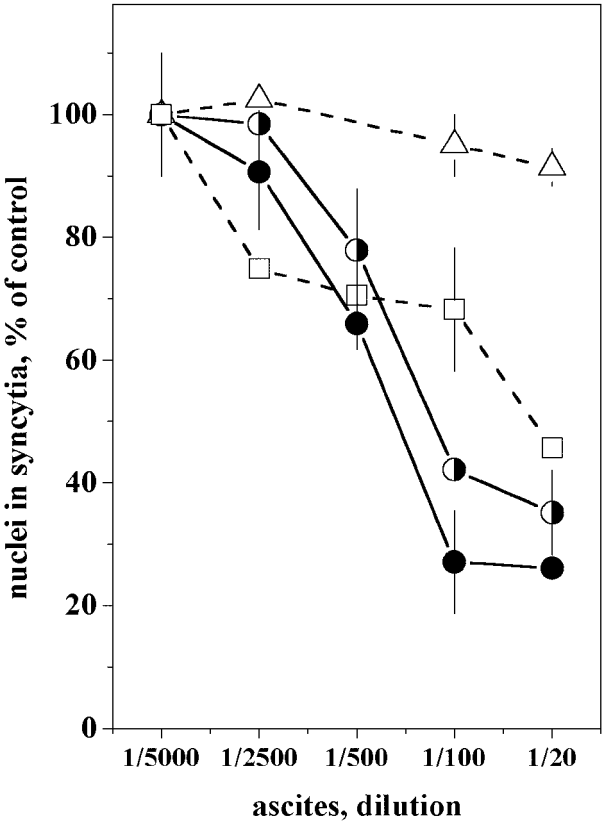


FIG. 6. **Inhibition of low pH-dependent syncytia formation in pG gene-transfected EPC cells by anti-peptide Abs.** EPC cells in 24-well plates were transfected with 0.6 $\mu$g of the pG containing plasmid G3-pcDNAI/Amp by using Fugene. Next day, the EPC monolayers were incubated 30 min at pH 6 in the presence of increasing concentrations of Abs (ascites dilutions), washed with cell culture medium, and after 2 h fixed with 1% glutaraldehyde and stained with Giemsa. The percentage of nuclei in syncytia in the absence of Abs (control) was 25.3 ± 6.2% ($n$ = 3). Results are expressed in percentage of the control by the following formula: number of nuclei in syncytia in the presence of Abs/number of nuclei in syncytia in the absence of Abs × 100. Averages and S.D. values from two experiments are represented except from six experiments for anti-fragment 11. ●, anti-fragment 11; ◑, anti-p2; △,anti-p3; □, anti-p4.

theoretical expectations mentioned above for an internal fusion domain. On the other hand, if p2 penetrates the hydrophobic part of the membrane with a $\beta$-sheet extended structure (1), it has to carry with it both the p3 and the disulfide-bound putative fusion domain, while according to the results obtained, both p9 and p4 should remain outside the membrane.

*Comparison of Fragment 11 Sequences in Other VHSV and*

*Rhabdoviruses*—Only six amino acid positions in the fragment 11 sequences from eight VHSV isolates showed variation. Most of them were conservative (I71T, T80A, R81K, R81Q, T90N, A96V, and S97N), demonstrating the highly conserved nature of these sequences among different strains of VHSV. On the other hand, there were no amino acid identities in the fragment 11-like sequences from 14 animal rhabdoviruses except the highly conserved cysteine-proline $C_IP$ ($Cys^{64}$ and $Pro^{65}$ in VHSV), and a glycine ($Gly^{98}$ in VHSV) situated at the end of the fragment 11-like sequence. All of the fragment 11-like sequences were found between two highly conserved cysteines, $C_I$ ($C_I$ bridged to $C_{XII}$, which in VHSV corresponded to $Cys^{64}$–$Cys^{315}$) and $C_{II}$ or $C_{III}$ ($C_{III}$ bridged to $C_V$, which in VHSV corresponded to $Cys^{110}$–$Cys^{152}$). $C_{II}$ was absent in cold water fish rhabdoviruses, and $C_{III}$ was absent in rabies-like rhabdoviruses. The disulfide bridge between $C_{III}$ and $C_V$ (or between $C_{II}$ and $C_{IV}$ in rabies-like viruses) brings together both putative phospholipid-binding and fusion domains in all rhabdoviruses.

*Main Conclusions and Future Work*—In contrast to all of the pG segments studied, only fragment 11 when added at low pH was able to induce syncytia or to produce significant translocation of PS, suggesting a major participation of fragment 11 domain in VHSV fusion. Comparison of the effects of mutations in both fragment 11 and in the putative fusion domains (3, 21) of VHSV would assess its relative importance during fusion. On the other hand, the fragment 11 capacity to disrupt membranes only at low pH and the presence of its amino- and carboxyl-terminal positive charges might serve particular purposes such as serving as a vehicle for DNA transfection (experiments in progress).

*Acknowledgments*—Thanks are due to J. P. Coll for typing, to Nuria Illera for technical assistance, to Dr. A. Benmansour for providing unpublished VHSV pG sequences, and to Dr. R. Blasco for critically reading the manuscript.

REFERENCES

1. Nuñez, E., Fernandez, A. M., Estepa, A., Gonzalez-Ros, J. M., Gavilanes, F., and Coll, J. M. (1998) *Virology* **243,** 322–330
2. Estepa, A., and Coll, J. M. (1996) *Virology* **216,** 60–70
3. Walker, P. J., and Kongsuwan, K. (1999) *J. Gen. Virol.* **80,** 1211–1220
4. Einer-Jensen, K., Krogh, T. N., Roepstorff, P., and Lorenzen, N. (1998) *J. Virol.* **72,** 10189–10196
5. Coll, J. M. (1995) *Virus Genes* **10,** 107–114
6. Coll, J. M. (1995) *Arch. Virol.* **140,** 827–851
7. Gaudin, Y., Ruigrok, R. W. H., Knossow, M., and Flamand, A. (1993) *J. Virol.* **67,** 1365–1372
8. Gaudin, Y., Tuffereau, C., Durrer, P., Brunner, J., Flamand, A., and Ruigrok, R. (1999) *Mol. Membr. Biol.* **16,** 21–31
9. Fredericksen, B. L., and Whitt, M. A. (1996) *Virology* **217,** 49–57
10. Shokralla, S., He, Y., Wanas, E., and Ghosh, H. P. (1998) *Virology* **242,** 39–50
11. Doms, R. W., Keller, D. S., Helenius, A., and Balch, W. E. (1987) *J. Cell Virol.* **105,** 1957–1969
12. Zhang, L., and Ghosh, H. P. (1994) *J. Virol.* **68,** 2186–2193
13. Flamand, A., Raux, H., Gaudin, Y., and Ruigrok, R. W. H. (1993) *Virology* **194,** 302–313
14. Delos, S. E., Gilbert, J. M., and White, J. M. (2000) *J. Virol.* **7,** 1686–1693
15. Estepa, A., and Coll, J. M. (1996) *J. Virol. Methods* **61,** 37–45
16. Coll, J. M. (1997) *Arch. Virol.* **142,** 2089–2097
17. Bearzotti, M., Delmas, B., Lamoureux, A., Loustau, A. M., Chilmonczyk, S., and Bremont, M. (1999) *J. Virol.* **73,** 7703–7709
18. Coll, J. M. (1999) *Recent Res. Dev. Virol.* **1,** 75–83
19. Estepa, A., and Coll, J. M. (1997) *Dis. Aquatic Organisms* **28,** 185–189
20. Lecocq-Xhonneux, F., Thiry, M., Dheur, I., Rossius, M., Vanderheijden, N., Martial, J., and DeKinkelin, P. (1994) *J. Gen. Virol.* **75,** 1579–1587
21. Gaudin, Y., DeKinkelin, P., and Benmansour, A. (1999) *J. Gen. Virol.* **80,** 1221–1229
22. Schulz, G. E., and Schimer, R. H. (eds) (1984) *Principles of Protein Structure*, p. 2, Springer-Verlag, New York
23. Thiry, M., Lecoq-Xhonneux, F., Dheur, I., Renard, A., and Kinkelin, D. (1991) *Biochim. Biophys. Acta* **1090,** 345–347
24. LeBerre, M., De Kinkelin, P., and Metzger, A. (1977) *Bull. Office Int. Epizooties* **87,** 391–393
25. Basurco, B., Sanz, F., Marcotegui, M. A., and Coll, J. M. (1991) *Arch. Virol.* **119,** 153–163
26. Lorenzo, G., Estepa, A., and Coll, J. M. (1996) *J. Virol. Methods* **58,** 1–6
27. Estepa, A., Fernandez-Alonso, M., and Coll, J. M. (1999) *Virus Res.* **63,** 27–34
28. Budker, V., Gurevich, V., Hagstrom, J. E., Bortzov, F., and Wolff, J. A. (1996) *Nat. Biotechnol.* **14,** 760–764
29. Perez, L., Estepa, A., and Coll, J. M. (1998) *J. Virol. Methods* **76,** 1–8
30. Coll, J. M. (1989) *J. Immunol. Methods* **104,** 219–222
31. Sanz, F. A., and Coll, J. M. (1992) *Am. J. Vet. Res.* **53,** 897–903
32. Carneiro, F. A., Ferradosa, A. S., and Da Poian, A. T. (2001) *J. Biol. Chem.* **276,** 62–67
33. Fernandez-Alonso, M., Alvarez, F., Estepa, A., Blasco, R., and Coll, J. M. (1999) *J. Fish Dis.* **22,** 237–241
34. Lopez, A., Fernandez-Alonso, M., Rocha, A., Estepa, A., and Coll, J. M. (2001) *Biotechnol. Lett.* **23,** 481–487
35. Bearzotti, M., Monnier, A. F., Vende, P., Grosclaude, J., DeKinkelin, P., and Benmansour, A. (1995) *Vet. Res.* **26,** 413–422
36. Lenard, J. (1993) *Viral Fusion Mechanisms* (Bentz, J., ed) pp. 425–435, CRC Press, Inc., Boca Raton, FL
37. Odell, D., Wanas, E., Yan, J., and Ghosh, H. P. (1997) *J. Virol.* **71,** 7996–8000